

## ARTICLE

# Infrared Photodissociation Spectroscopy of Boron Carbonyl Cation Complexes<sup>†</sup>

Jia-ye Jin, Guan-jun Wang, Ming-fei Zhou\*

*Collaborative Innovation Center of Chemistry for Energy Materials, Department of Chemistry, Shanghai Key Laboratory of Molecular Catalysts and Innovative Materials, Fudan University, Shanghai 200433, China*

(Dated: Received on November 25, 2015; Accepted on December 8, 2015)

The boron carbonyl cation complexes  $B(CO)_3^+$ ,  $B(CO)_4^+$  and  $B_2(CO)_4^+$  are studied by infrared photodissociation spectroscopy and theoretical calculations. The  $B(CO)_4^+$  ions are characterized to be very weakly bound complexes involving a  $B(CO)_3^+$  core ion, which is predicted to have a planar  $D_{3h}$  structure with the central boron retaining the most favorable 8-electron configuration. The  $B_2(CO)_4^+$  cation is determined to have a planar  $D_{2h}$  structure involving a B–B one and half bond. The analysis of the B–CO interactions with the EDA–NOCV method indicates that the  $OC \rightarrow B$   $\sigma$  donation is stronger than the  $B \rightarrow CO$   $\pi$  back donation in both ions.

**Key words:** Boron carbonyl, Donor-acceptor bonding, Infrared photodissociation spectroscopy, Theoretical calculations

## I. INTRODUCTION

Carbon monoxide is one of the most important ligand in inorganic and organometallic chemistry [1]. It can bind to a host of neutral and charged transition metal centers in forming diverse metal carbonyl complexes, in which carbon monoxide serves either as a two-electron donor in an end-on coordinated fashion or as a four-electron or even six-electron donor in the bridge bonded modes [2–11]. Carbon monoxide can also coordinate with some main-group elements in forming main group carbonyl complexes [12, 13]. Homoleptic mono- and dicarbonyl complexes of main group elements with end-on bonded carbonyl ligands have been prepared and spectroscopically characterized either in low-temperature noble gas matrices or in the gas phase [12–38]. These carbonyl complexes are usually not stable at ambient conditions with the exception of  $[C(CO)_2]$  and  $[N(CO)_2]^+$  which have been crystallographically characterized [36–38].

In the case of boron, the electron deficient boron species are able to coordinate one CO ligand in forming the closed-shell carbonyl borane  $H_3BCO$  and related derivatives, which are well-known stable carbonyl compounds [39–43]. Boron carbonyl species such as  $BCO$ ,  $B(CO)_2$ ,  $B(CO)_2^-$ ,  $OCBBO$ ,  $BBO$  and  $B_4(CO)_2$  were identified as products from the reac-

tions of thermal- or laser-evaporated boron atoms with CO in solid argon [44–50]. The  $OCBBO$  molecule was characterized to be a boron-boron triple bonded species [48]. Both  $BBO$  and  $B_4(CO)_2$  are  $\sigma$ - $\pi$  diradicals [49, 50]. Bonding analysis suggests that the linear closed-shell  $B(CO)_2^-$  anion should be considered as a donor-acceptor bonding complex rather than a cumulene  $O=C=B(-)=C=O$  molecule with electron sharing bonding [47]. Very recently, a rare example of a boron dicarbonyl complex  $[(RB)(CO)_2]$  (R being a bulky aryl group) with two terminal carbonyl ligands which is stable under ambient conditions has been reported [51]. The chemical behavior shows typical features of carbonyl complexes which are known from transition metal carbonyls. Boron carbonyl cation complexes are not known so far. Here we report a combined infrared photodissociation spectroscopy and theoretical study on boron carbonyl cation complexes  $B(CO)_3^+$  and  $B_2(CO)_4^+$  in the gas phase.

## II. EXPERIMENTAL AND THEORETICAL METHODS

The boron carbonyl cation complexes are generated in the gas phase using a pulsed laser vaporization/supersonic expansion ion source as described previously [52, 53]. Bulk targets compressed from isotopically-enriched  $^{10}B$  and  $^{11}B$  powders were used. The ions are produced from the laser vaporization process in expansions of helium seeded with 2%–5% CO using a pulsed valve (General Valve, Series 9) at 0.5–1.0 MPa backing pressure. After free expansion and cooling, the cations are skimmed into a second chamber where they are pulse-extracted into a Wiley-

<sup>†</sup>Part of the special issue for “the Chinese Chemical Society’s 14th National Chemical Dynamics Symposium”.

\*Author to whom correspondence should be addressed. E-mail: mfmzhou@fudan.edu.cn

McLaren type time-of-flight mass spectrometer. The cations of interest are mass selected and decelerated into the extraction region of a second collinear time-of-flight mass spectrometer, where they are dissociated by a tunable IR laser. The tunable IR laser used is generated by a KTP/KTA//AgGaSe<sub>2</sub> optical parametric oscillator/amplifier system (OPO/OPA, Laser Vision) pumped by a Continuum Surelite EX Nd:YAG laser, producing about 1.0–2.5 mJ/pulse in the range of 1800–2400 cm<sup>-1</sup>. The ion density is too low for infrared absorption spectroscopy, thus, the infrared photodissociation spectroscopy is employed to record the vibrational spectra. Resonant absorption leads to fragmentation of the ion complex. The infrared photodissociation spectrum is obtained by monitoring the yield of the fragment ion as a function of the dissociation IR laser wavelength and normalizing to parent ion signal.

The geometry optimizations have been carried out without symmetry constraints at the B3LYP level using the aug-cc-pVTZ basis sets [54–56]. The harmonic vibrational frequencies were calculated with analytic second derivatives. These calculations were performed using the Gaussian 09 program [57]. The gradient corrected BP86 functional in conjunction with uncontracted Slater-type orbitals (STOs) as basis functions was used for the bonding analyses [58–60]. The latter basis sets for all elements have triple- $\xi$  quality augmented by one set of polarization functions (ADF-basis set TZP). An auxiliary set of s, p, d, f, and g STOs was used to fit the molecular densities and to represent the Coulomb and exchange potentials accurately in each SCF cycle. The BP86/TZP calculations were performed using the B3LYP/aug-cc-pVTZ optimized geometries with the program package ADF2014.10 [61].

### III. RESULTS AND DISCUSSION

The mass spectrum of boron carbonyl cation complexes in the  $m/z$  range of 60–150 from the laser evaporation of a <sup>10</sup>B-enriched target in expansions of helium gas seeded with 5% CO is shown in Fig.1(a). Although the mass spectra depend strongly on the parameters of the ion source such as vaporization laser power, He and CO stagnation pressures and timing, the peaks corresponding to <sup>10</sup>B(CO)<sub>3</sub><sup>+</sup> ( $m/z=94$ ) and <sup>10</sup>B<sub>2</sub>(CO)<sub>4</sub><sup>+</sup> ( $m/z=132$ ) are always the most intense peaks, suggesting that these cations are formed preferentially with high stability. The mass spectrum from the experiments with the <sup>11</sup>B-enriched target is shown in Fig.1(b). The most intense peaks shifted to  $m/z=95$  and 134, corresponding to the <sup>11</sup>B(CO)<sub>3</sub><sup>+</sup> and <sup>11</sup>B<sub>2</sub>(CO)<sub>4</sub><sup>+</sup> ions, respectively.

The B(CO)<sub>3</sub><sup>+</sup> cations are mass-selected and subjected to infrared photodissociation. It is found that the B(CO)<sub>3</sub><sup>+</sup> cations dissociate via losing a CO ligand when excited with infrared light in the 2140–2150 cm<sup>-1</sup> frequency region but the dissociation efficiency (less

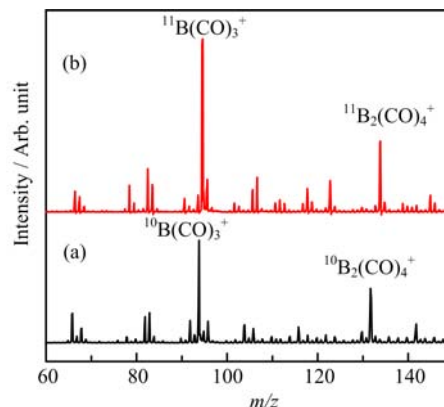


FIG. 1 Mass spectra of the boron carbonyl cation complexes formed by pulsed laser vaporization of a target in an expansion of helium doped with carbon monoxide. (a) <sup>10</sup>B and (b) <sup>11</sup>B.

than 0.5%) is too low to achieve an effective spectrum. This suggests that the B(CO)<sub>3</sub><sup>+</sup> cations are very stable species with quite high CO binding energy as expected, as it satisfies the octet rule. In contrast to B(CO)<sub>3</sub><sup>+</sup>, the B(CO)<sub>4</sub><sup>+</sup> cation complexes are able to dissociate via loss of a CO ligand with very high efficiency (>50%), indicating that B(CO)<sub>4</sub><sup>+</sup> is a very weakly bound complex. This confirms our expectation that B(CO)<sub>3</sub><sup>+</sup> is a fully coordinated ion and the fourth CO in B(CO)<sub>4</sub><sup>+</sup> is a weakly bound external carbonyl ligand. Therefore, the B(CO)<sub>4</sub><sup>+</sup> cation can be regarded as a CO “tagged” cation complex involving a B(CO)<sub>3</sub><sup>+</sup> core ion. The infrared photodissociation spectrum of B(CO)<sub>4</sub><sup>+</sup> represents the spectrum of the B(CO)<sub>3</sub><sup>+</sup> core ion that is weakly perturbed by the tagged CO ligand. The tagging effect is expected to change the position of the B(CO)<sub>3</sub><sup>+</sup> band only slightly as discussed previously [62–64]. The infrared photodissociation spectra of <sup>11</sup>B(CO)<sub>4</sub><sup>+</sup> and <sup>10</sup>B(CO)<sub>4</sub><sup>+</sup> in the C–O stretching frequency region are shown in Fig.2. The spectrum of <sup>10</sup>B(CO)<sub>4</sub><sup>+</sup> (Fig.2(a)) exhibits a very strong band centered at 2145 cm<sup>-1</sup> along with a weak band at 2178 cm<sup>-1</sup>. The 2145 cm<sup>-1</sup> band is just 2 cm<sup>-1</sup> blue-shifted from the frequency of gas phase carbon monoxide (2143 cm<sup>-1</sup>). This band can be attributed to the antisymmetric CO stretching vibrations of the <sup>10</sup>B(CO)<sub>3</sub><sup>+</sup> core ion. The much weak band at 2178 cm<sup>-1</sup> is assigned to the CO stretching vibration of the weakly tagged CO ligand, consistent with previous observations for other weakly bound metal ion carbonyls [64–66]. The same bands were also observed in the spectrum of <sup>11</sup>B(CO)<sub>4</sub><sup>+</sup> as shown in Fig.2(b). The band positions are essentially the same indicating that the corresponding vibrational modes are pure CO stretching vibrations with negligible boron involvement. Besides 2145 and 2178 cm<sup>-1</sup> bands, additional weak bands at 2214 and 2259 cm<sup>-1</sup> were observed in the spectrum of <sup>11</sup>B(CO)<sub>4</sub><sup>+</sup>. Both bands are located in the frequency range suitable for the symmet-

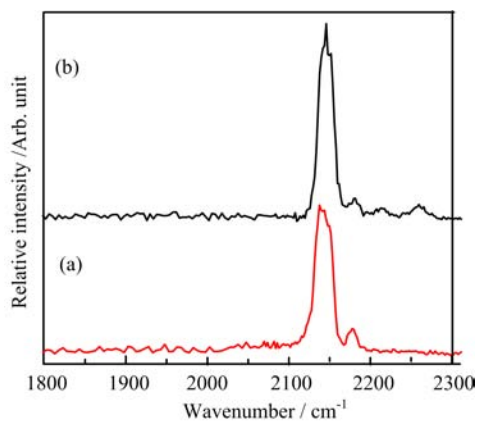


FIG. 2 The experimental infrared photodissociation spectra of the (a)  $^{10}\text{B}(\text{CO})_4^+$  and (b)  $^{11}\text{B}(\text{CO})_4^+$  cation complexes in the CO stretching frequency region.

ric CO stretching vibrations. We tentatively assign the  $2259\text{ cm}^{-1}$  band to the symmetric stretching vibration of the  $^{11}\text{B}(\text{CO})_3^+$  core ion and the  $2214\text{ cm}^{-1}$  band to a combination or an overtone level that is in Fermi resonance with the symmetric CO stretching fundamental. When  $^{11}\text{B}$  is substituted by  $^{10}\text{B}$ , the two levels are no long close enough to show Fermi resonance, therefore, both bands were not observed in the spectrum of  $^{10}\text{B}(\text{CO})_4^+$ .

The  $\text{B}_2(\text{CO})_4^+$  cation is able to dissociate via loss of a CO ligand under focused IR laser irradiation. The parent ions can be depleted by about 5% at the laser pulse energy of  $1.4\text{ mJ/pulse}$  at  $2108\text{ cm}^{-1}$ . The infrared photodissociation spectrum of  $^{10}\text{B}_2(\text{CO})_4^+$  is shown in Fig.3. The spectrum exhibits two bands centered at 2108 and  $2152\text{ cm}^{-1}$ .

We carried out high-level calculations in order to validate the identify of the cations and to analyze their electronic structures. The theoretically predicted geometries of  $\text{B}(\text{CO})_3^+$  and  $\text{B}(\text{CO})_4^+$  are shown in Fig.4. The  $\text{B}(\text{CO})_3^+$  cation has a  $^1\text{A}'_1$  ground state with planar  $\text{D}_{3h}$  symmetry. The calculations indicate that the CO bond distances in  $\text{B}(\text{CO})_3^+$  ( $1.127\text{ \AA}$ ) is slightly shorter than that of free CO calculated at the same level ( $1.128\text{ \AA}$ ). As shown in Fig.5, the highest doubly occupied molecular orbital (HOMO,  $a'_2$ ) is primarily a central B2p orbital, which comprises significant B2p to CO  $2\pi^*$  back bonding. Therefore, the  $^1\text{A}'_1$  ground state  $\text{B}(\text{CO})_3^+$  cation correlates to an electronic excited singlet state  $\text{B}^+$  with the associated valence electronic configuration of  $2s^0, 2p(\sigma)^0, 2p(\pi)^2, 2p(\pi')^0$ . The  $^{11}\text{B}(\text{CO})_3^+$  cation with  $\text{D}_{3h}$  symmetry has only one IR active antisymmetric CO stretching mode calculated at  $2223\text{ cm}^{-1}$ , which is doubly degenerate. This mode for  $^{10}\text{B}(\text{CO})_3^+$  is predicted at  $2224\text{ cm}^{-1}$ . The symmetric stretching mode is predicted at  $2317\text{ cm}^{-1}$  which is IR inactive. Consistent with the experimental observations, the  $\text{B}(\text{CO})_4^+$  cation was predicted to be a weakly bound complex as the predicted B–CO distance of the fourth CO is

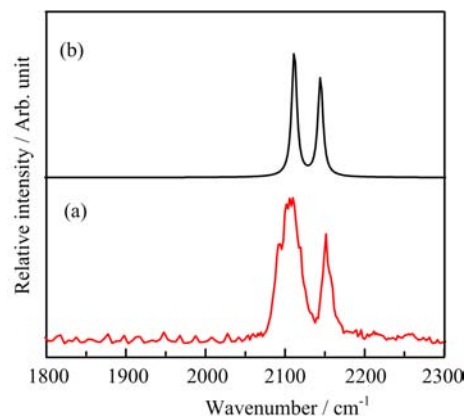


FIG. 3 Experimental and simulated IR spectra of  $^{10}\text{B}_2(\text{CO})_4^+$  in the CO stretching frequency region. The experimental spectrum (a) was measured by monitoring the CO fragmentation channel leading to the formation of  $\text{B}_2(\text{CO})_3^+$ . The simulated spectrum (b) was obtained from scaled (0.971) harmonic frequencies and intensities calculated at the B3LYP/aug-cc-pVTZ level.

TABLE I Observed and calculated (harmonic, unscaled) CO stretching frequencies ( $\text{cm}^{-1}$ ) of the  $^{10}\text{B}(\text{CO})_4^+$  and  $^{10}\text{B}_2(\text{CO})_4^+$  ions.

Fragments	Expt.	Calc. <sup>a</sup>
$\text{B}(\text{CO})_3^+$		2317(0)
		2224(987, 978)
$\text{B}(\text{CO})_4^+$	2178	2316(0)
	2145	2254(35)
$\text{B}_2(\text{CO})_4^+$		2224(961), 2218(1024)
		2271(0)
	2152	2208(1703)
	2108	2175(2162)
		2151(0)

<sup>a</sup> The intensities are listed in parentheses in km/mol.

quite large with the geometry of the  $\text{B}(\text{CO})_3^+$  core ion being essentially the same as the free cation. Due to symmetry reduction by CO coordination, the double degeneracy of the antisymmetric CO stretching mode of  $\text{B}(\text{CO})_3^+$  is lifted, and the E mode splits into two distinct modes. Calculations at the B3LYP level show very small mode split of  $6\text{ cm}^{-1}$ , which cannot be well-resolved experimentally.

The  $\text{B}_2(\text{CO})_4^+$  cation was predicted to have a doublet ground state ( $^2\text{B}_{2g}$ ) with planar  $\text{D}_{2h}$  symmetry. The B–B bond length is predicted to be  $1.638\text{ \AA}$ , which is intermediate between typical B–B single bond and double bond [67]. The cation with planar  $\text{D}_{2h}$  structure has four CO stretching modes with only two of them are IR active, which are calculated to be  $2175$  and  $2208\text{ cm}^{-1}$  at the B3LYP/aug-cc-pVTZ level. The

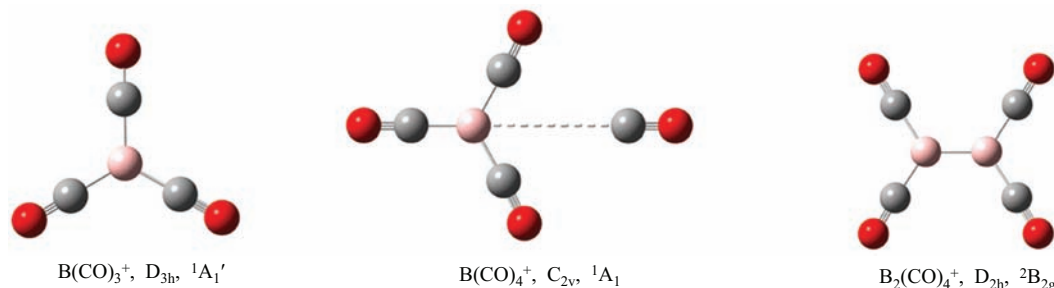


FIG. 4 Optimized structures of the  $B(CO)_3^+$ ,  $B(CO)_4^+$  and  $B_2(CO)_4^+$  cation complexes.

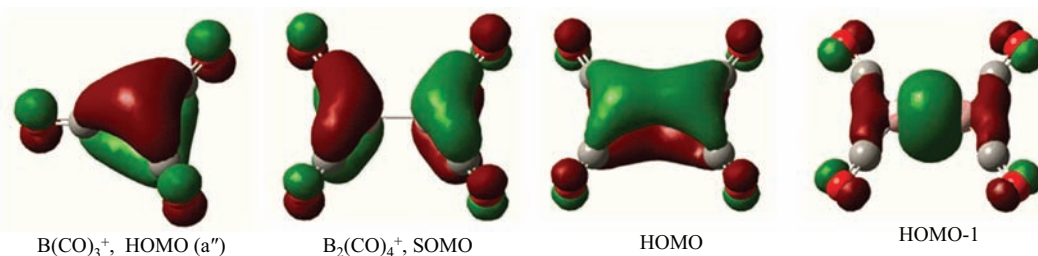


FIG. 5 Molecular orbital pictures of the highest doubly occupied (HOMO) of  $B(CO)_3^+$  and the singly occupied (SOMO) and highest doubly occupied orbitals (HOMO and HOMO-1) of  $B_2(CO)_4^+$ .

molecular orbital pictures shown in Fig.5 clearly indicate that the singly occupied (SOMO)  $b_{2g}$  MO is a B–B  $\pi$  antibonding orbital. The highest doubly occupied  $b_{3u}$  orbital (HOMO) is a B–B  $\pi$  bonding orbital. Both the  $b_{2g}$  and  $b_{3u}$  orbitals comprise substantial  $B_2^+$  to CO  $\pi^*$  back-donation. Both orbitals are highly delocalized involving two B and four C centers. The doubly occupied  $a_g$  molecular orbital (HOMO-1) is a B–B  $\sigma$  bonding orbital. The ground state  $B_2(CO)_4^+$  cation complex can thus be viewed as the interaction of a  $^2\Pi_g$  excited-state  $B_2^+$  and four CO's, which involves one B–B  $\sigma$  bond and a half B–B  $\pi$  bond.

The bond dissociation energies of  $B(CO)_3^+$ ,  $B(CO)_4^+$  and  $B_2(CO)_4^+$  are calculated. At the B3LYP level, the BDE of  $B(CO)_3^+$  is 79.5 kcal/mol with respect to the dissociation limit  $B(CO)_2^+(^1\Delta_g)+CO$  or 60.7 kcal/mol with respect to the ground state reactants:  $B(CO)_2^+(^3\Sigma_g)+CO$ . The dissociation energy of the tagged CO in  $B(CO)_4^+$  is calculated to be only 2.9 kcal/mol. The binding energy of  $B_2(CO)_4^+$  is 60.4 kcal/mol with respect to the dissociation limit  $B_2(CO)_3^+(^2B_1)+CO$  or 39.2 kcal/mol for the dissociation into the ground state  $B_2(CO)_3^+(^2B_2)$  and CO.

We analyze the nature of the donor-acceptor interactions in  $B(CO)_3^+$  and  $B_2(CO)_4^+$  with the EDA (energy decomposition analysis) in conjunction with the NOCV (natural orbitals for chemical valence) method [68], which gives a detailed insight into the bonding situation. The numerical results of the OC–B interactions in  $B(CO)_3^+$  and  $B_2(CO)_4^+$  at the BP86/TZP level are listed in Table II. The data show that both species have

TABLE II EDA-NOCV results of the chemical bonding in  $OC-B(CO)_2^+$  and  $OC-B_2(CO)_3^+$  at BP86/TZP. Energy values are given in kcal/mol.

	CO and $B(CO)_2^+$ ( $^1\Delta_g$ )	CO and $B_2(CO)_3^+$ ( $^2B_1$ )
$\Delta E_{\text{int}}$	–105.6	–91.9
$\Delta E_{\text{pauli}}$	108.2	136.9
$\Delta E_{\text{elstat}}$	–62.5	–71.3
$\Delta E_{\text{orb}}$	–151.3	–157.4
$\Delta E_{\text{orb}} \sigma$ donation	–104.2	–103.2
$\Delta E_{\text{orb}} \pi_{\perp}$	–31.1	–60.1
$\Delta E_{\text{orb}} \pi_{\parallel}$	–10.1	–14.2
$\Delta E_{\text{orb}(\text{rest})}$	–5.9	20.1

very similar orbital interaction energy ( $\Delta E_{\text{orb}}$ ). Further inspection of the orbital components of  $\Delta E_{\text{orb}}$  reveals that both species have very similar CO→B  $\sigma$  donation interaction, which is much stronger than the B→CO  $\pi$  back donation interactions. There is a large difference in the strength of the B→CO  $\pi$  back donation between the two complexes. The  $\pi$  contribution of  $\Delta E_{\text{orb}}(\pi_{\perp})+\Delta E_{\text{orb}}(\pi_{\parallel})$  in  $B_2(CO)_4^+$  is much larger than that in  $B(CO)_3^+$ . Figure 6 displays the deformation densities  $\Delta\rho(\sigma)$  and  $\Delta\rho(\pi)$  which are connected to the  $\sigma$  donation and  $\pi$  backdonation in  $B(CO)_3^+$  and  $B_2(CO)_4^+$ . The direction of the charge flow is indicated by the colors red→blue. The shape of  $\Delta\rho(\sigma)$  clearly indicates that the charge flow comes mainly from the lone-pair



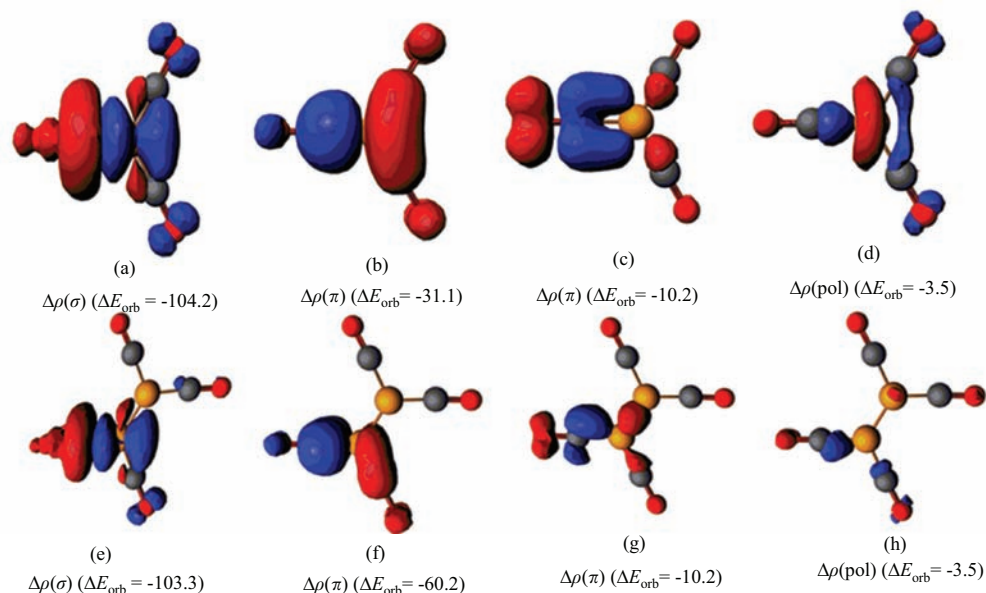


FIG. 6 Plot of deformation densities  $\Delta\rho$  of the pairwise orbital interactions and the associated interaction energies  $\Delta E_{\text{orb}}$  (in kcal/mol) between CO and  $\text{B}(\text{CO})_2^+$  or  $\text{B}_2(\text{CO})_3^+$  in  $\text{B}(\text{CO})_3^+$  and  $\text{B}_2(\text{CO})_4^+$ . The direction of charge flow is red $\rightarrow$ blue.

electrons at carbon to the boron atom. While the  $\pi$  backdonation leads to charge accumulation mainly at the carbon atom of CO.

#### IV. CONCLUSION

Boron carbonyl cation complexes are produced via a laser vaporization supersonic ion source in the gas phase. The cations of interest are each mass-selected and their infrared spectra are measured via infrared photodissociation spectroscopy in the carbonyl stretching frequency region. Density functional calculations have been performed and the calculated vibrational spectra are compared to the experimental data to identify the gas-phase structures of the ions. The  $\text{B}(\text{CO})_3^+$  and  $\text{B}_2(\text{CO})_4^+$  cations are the most intense peaks in the mass spectrum. The  $\text{B}(\text{CO})_3^+$  ion is too strongly bound to achieve an effective IR spectrum. In contrast, the  $\text{B}(\text{CO})_4^+$  ion dissociates very efficiently under IR irradiation. It is characterized to be a very weakly bound complex involving a  $\text{B}(\text{CO})_3^+$  core ion, which is predicted to have a planar  $D_{3h}$  structure with the central boron retaining the most favorable 8-electron configuration. The  $\text{B}_2(\text{CO})_4^+$  cation is determined to have a planar  $D_{2h}$  structure involving a B–B bond. Both the  $\text{B}(\text{CO})_3^+$  and  $\text{B}_2(\text{CO})_4^+$  ions have slightly red- or blue-shifted CO stretching frequencies with respect to free CO. The analysis of the B–CO interactions with the EDA–NOCV method indicates that the  $\text{OC}\rightarrow\text{B}$   $\sigma$  donation is stronger than the  $\text{B}\rightarrow\text{CO}$   $\pi$  back donation.

#### V. ACKNOWLEDGMENTS

The work was supported by the Ministry of Science and Technology of China (No.2013CB834603) and

the National Natural Science Foundation of China (No.21173053 and No.21433005).

- [1] F. A. Cotton, G. Wilkinson, C. A. Murillo, and M. Bochmann, *Advanced Inorganic Chemistry*, 6th Edn., New York: John Wiley, (1999).
- [2] G. Frenking and N. Fröhlich, *Chem. Rev.* **100**, 717 (2000).
- [3] M. F. Zhou, L. Andrews, and C. W. Bauschlicher Jr., *Chem. Rev.* **101**, 1931 (2001).
- [4] F. A. Cotton, B. A. Frenz, and L. Kruczynski, *J. Am. Chem. Soc.* **95**, 951 (1973).
- [5] M. Manassero, M. Sansoni, and G. Longoni, *J. Chem. Soc. Chem. Commun.* 919 (1976).
- [6] R. Colton and M. J. McCormick, *Coord. Chem. Rev.* **31**, 1 (1980).
- [7] L. Jiang and Q. Xu, *J. Am. Chem. Soc.* **127**, 42 (2005).
- [8] X. J. Zhou, J. M. Cui, Z. H. Li, G. J. Wang, Z. P. Liu, and M. F. Zhou, *J. Phys. Chem. A* **117**, 1514 (2013).
- [9] J. H. Osborne, A. L. Rheingold, and W. C. Trogler, *J. Am. Chem. Soc.* **107**, 6292 (1985).
- [10] X. J. Zhou, J. M. Cui, Z. H. Li, G. J. Wang, and M. F. Zhou, *J. Phys. Chem. A* **116**, 12349 (2012).
- [11] W. A. Herrmann, H. Biersack, M. L. Ziegler, K. Weidenhammer, R. Siegel, and D. Rehder, *J. Am. Chem. Soc.* **103**, 1692 (1981).
- [12] A. J. Bridgeman, *Inorg. Chim. Acta.* **321**, 27(2001).
- [13] H. J. Himmel, A. J. Downs, and T. M. Greene, *Chem. Rev.* **102**, 4191 (2002).
- [14] L. Andrews, T. J. Tague, and G. P. Kushto, *Inorg. Chem.* **34**, 2952 (1995).
- [15] P. H. Kasai and P. M. Jones, *J. Am. Chem. Soc.* **106**, 8018 (1984).
- [16] J. H. B. Chenier, C. A. Hampson, J. A. Howard, B. Mile, and R. Sutcliffe, *J. Phys. Chem.* **90**, 1524 (1986).
- [17] C. Xu, L. Manceron, and J. P. Perchard, *J. Chem. Soc., Faraday Trans.* **89**, 1291 (1993).

- [18] Q. Y. Kong, M. H. Chen, J. Dong, Z. H. Li, K. N. Fan, and M. F. Zhou, *J. Phys. Chem. A* **106**, 11709 (2002).
- [19] L. N. Zhang, J. Dong, M. F. Zhou, and Q. Z. Qin, *J. Chem. Phys.* **113**, 10169 (2000).
- [20] P. H. Kasai and P. M. Jones, *J. Phys. Chem.* **89**, 2019 (1985).
- [21] J. A. Howard, R. Sutcliffe, C. A. Hampson, and B. Mile, *J. Phys. Chem.* **90**, 4268 (1986).
- [22] H. J. Himmel, A. J. Downs, J. C. Greene, and T. M. Greene, *J. Phys. Chem. A* **104**, 3642 (2000).
- [23] W. G. Hatton, N. P. Hacker, and P. H. Kasai, *J. Phys. Chem.* **93**, 1328 (1989).
- [24] R. R. Lembke, R. F. Ferrante, and W. Weltner, *J. Am. Chem. Soc.* **99**, 416 (1977).
- [25] M. F. Zhou, L. Jiang, and Q. Xu, *J. Chem. Phys.* **121**, 10474 (2004).
- [26] A. Feltrin, S. N. Cesaro, and F. Ramondo, *Vib. Spectrosc.* **10**, 139 (1996).
- [27] M. F. Zhou, L. Jiang, and Q. Xu, *J. Phys. Chem. A* **109**, 3325 (2005).
- [28] A. Bos, *J. Chem. Soc. Chem. Commun.* **1**, 26 (1972).
- [29] L. N. Zhang, J. Dong, and M. F. Zhou, *J. Chem. Phys.* **113**, 8700 (2000).
- [30] L. Jiang and Q. Xu, *Bull. J. Chem. Soc. Jpn.* **79**, 857 (2006).
- [31] L. Jiang and Q. Xu, *J. Chem. Phys.* **122**, 034505 (2005).
- [32] L. N. Zhang, J. Dong, and M. F. Zhou, *Chem. Phys. Lett.* **335**, 334 (2001).
- [33] A. J. Bridgeman, N. Harris, and N. A. Young, *Chem. Commun.* **14**, 1241 (2000).
- [34] T. Liang, S. D. Flynn, A. M. Morrison, and G. E. Doublerly, *J. Phys. Chem. A* **115**, 7437 (2011).
- [35] A. D. Brathwaite and M. A. Duncan, *J. Phys. Chem. A* **116**, 1375 (2012).
- [36] A. Ellern, T. Drews, and L. Seppelt, *Z. Anorg. Allg. Chem.* **627**, 73 (2001).
- [37] R. Tonner and G. Frenking, *Chem. Eur. J.* **14**, 3260 (2008).
- [38] I. Bernhardt, T. Drews, and K. Seppelt, *Angew. Chem. Int. Ed.* **38**, 2232 (1999).
- [39] A. B. Burg and H. I. Schlesinger, *J. Am. Chem. Soc.* **59**, 780 (1937).
- [40] A. Terheiden, E. Bernhardt, H. Willner, and F. Aubke, *Angew. Chem. Int. Ed.* **41**, 799 (2002).
- [41] M. Finze, E. Bernhardt, A. Terheiden, M. Berkei, H. Willner, D. Christen, H. Oberhammer, and F. Aubke, *J. Am. Chem. Soc.* **124**, 15385 (2002).
- [42] M. Gerken, G. Pawelke, E. Bernhardt, and H. Willner, *Chem. Eur. J.* **16**, 7527 (2010).
- [43] A. Fukazawa, J. L. Dutton, C. Fan, L. G. Mercier, A. Y. Houghton, Q. Wu, W. E. Piers, and M. Parvez, *Chem. Sci.* **3**, 1814 (2012).
- [44] Y. M. Hamrick, R. J. V. Zee, J. T. Godbout, W. Weltner, W. J. Lauderdale, J. F. Stanton, and R. J. Bartlett, *J. Phys. Chem.* **95**, 2840 (1991).
- [45] T. R. Burkholder and L. Andrews, *J. Phys. Chem.* **96**, 10195 (1992).
- [46] M. F. Zhou, N. Tsumori, L. Andrews, and Q. Xu, *J. Phys. Chem. A* **107**, 2458 (2003).
- [47] Q. N. Zhang, W. L. Li, C. Xu, M. H. Chen, M. F. Zhou, J. Li, D. M. Andrada, and G. Frenking, *Angew. Chem. Int. Ed.* **54**, 11078 (2015).
- [48] M. F. Zhou, N. Tsumori, Z. H. Li, K. N. Fan, L. Andrews, and Q. Xu, *J. Am. Chem. Soc.* **124**, 12936 (2002).
- [49] M. F. Zhou, Z. X. Wang, P. R. Schleyer, and Q. Xu, *Chem. Phys. Chem.* **4**, 763 (2003).
- [50] M. F. Zhou, Q. Xu, Z. X. Wang, and P. R. Schleyer, *J. Am. Chem. Soc.* **124**, 14854 (2002).
- [51] H. Braunschweig, R. D. Dewhurst, F. Hupp, M. Nutz, K. Radacki, C. W. Tate, A. Vargas, and Y. Ye, *Nature* **522**, 327 (2015).
- [52] G. J. Wang, C. X. Chi, X. P. Xing, C. J. Ding, and M. F. Zhou, *Sci. China Chem.* **57**, 172 (2014).
- [53] G. J. Wang, C. X. Chi, J. M. Cui, X. P. Xing, and M. F. Zhou, *J. Phys. Chem. A* **116**, 2484 (2012).
- [54] A. D. Becke, *J. Chem. Phys.* **98**, 5648 (1993).
- [55] C. Lee, W. Yang, and R. G. Parr, *Phys. Rev. B* **37**, 785 (1988).
- [56] D. E. Woon and T. H. Dunning Jr., *J. Chem. Phys.* **100**, 2975 (1994).
- [57] M. J. Frisch, G. W. Trucks, H. B. Schlegel, G. E. Scuseria, M. A. Robb, J. R. Cheeseman, G. Scalmani, V. Barone, B. Mennucci, G. A. Petersson, H. Nakat-suji, M. Caricato, X. Li, H. P. Hratchian, A. F. Izmaylov, J. Bloino, G. Zheng, J. L. Sonnenberg, M. Hada, M. Ehara, K. Toyota, R. Fukuda, J. Hasegawa, M. Ishida, T. Nakajima, Y. Honda, O. Kitao, H. Nakai, T. Vreven, J. A. Montgomery Jr., J. E. Peralta, F. Ogliaro, M. Bearpark, J. J. Heyd, E. Brothers, K. N. Kudin, V. N. Staroverov, R. Kobayashi, J. Normand, K. Raghavachari, A. Rendell, J. C. Burant, S. S. Iyengar, J. Tomasi, M. Cossi, N. Rega, N. J. Millam, M. Klene, J. E. Knox, J. B. Cross, V. Bakken, C. Adamo, J. Jaramillo, R. Gomperts, R. E. Stratmann, O. Yazyev, A. J. Austin, R. Cammi, C. Pomelli, J. W. Ochterski, R. L. Martin, K. Morokuma, V. G. Zakrzewski, G. A. Voth, P. Salvador, J. J. Dannenberg, S. Dapprich, A. D. Daniels, Ö. Farkas, J. B. Foresman, J. V. Ortiz, J. Cioslowski, and D. J. Fox, *Gaussian 09, Revision A02*, Pittsburgh, PA: Gaussian, Inc., (2009).
- [58] A. D. Becke, *Phys. Rev. A* **38**, 3098 (1988).
- [59] J. P. Perdew, *Phys. Rev. B* **33**, 8822 (1986).
- [60] J. G. Snijders, E. J. Baerends, and P. Vernoojs, *At. Data Nucl. Data Tables* **26**, 483 (1981).
- [61] G. Te Velde, F. M. Bickelhaupt, E. J. Baerends, C. Fonseca Guerra, S. J. A. Van Gisbergen, J. G. Snijders, and T. Ziegler, *J. Comput. Chem.* **22**, 931 (2001).
- [62] M. Okumura, L. I. Yeh, J. D. Myers, and Y. T. Lee, *J. Chem. Phys.* **85**, 2328 (1986).
- [63] W. H. Robertson and M. A. Johnson, *Annu. Rev. Phys. Chem.* **54**, 173 (2003).
- [64] A. M. Ricks, Z. E. Reed, and M. A. Duncan, *J. Mol. Spectrosc.* **266**, 63 (2011).
- [65] G. J. Wang, J. M. Cui, C. X. Chi, X. J. Zhou, Z. H. Li, X. P. Xing, and M. F. Zhou, *Chem. Sci.* **3**, 3272 (2012).
- [66] J. M. Cui, G. J. Wang, X. J. Zhou, C. X. Chi, Z. H. Li, Z. P. Liu, and M. F. Zhou, *Phys. Chem. Chem. Phys.* **15**, 10224 (2013).
- [67] P. Pyykkö and M. Atsumi, *Chem. Eur. J.* **15**, 12770 (2009).
- [68] M. P. Mitoraj, A. Michalak, and T. Ziegler, *J. Chem. Theory Comput.* **5**, 962 (2009).